Quaternary International 313-314 (2013) 130–136

Contents lists available at ScienceDirect

Quaternary International

journal homepage: www.elsevier.com/locate/quaint

Spatio-temporal changes in free-air freezing level heights in Northwest China, 1960–2012

Xiaoyan Huang [a,*], Shengjie Wang [b], Jinsong Wang [a], Yaohui Li [a], Jianying Feng [a], Kai Zhang [a]

[a] Lanzhou Institute of Arid Meteorology of China Meteorological Administration, Key Laboratory of Arid Climate Change and Reducing Disaster of Gansu Province, Key Open Laboratory of Arid Climate Change and Reducing Disaster of China Meteorological Administration, Lanzhou 730020, China
[b] College of Geography and Environmental Science, Northwest Normal University, Lanzhou 730070, China

ARTICLE INFO

Article history:
Available online 20 September 2013

ABSTRACT

Based on the NCEP/NCAR reanalysis, the long-term changes in free-air freezing level height (FLH) in Northwest China during 1960–2012 were investigated. The results indicated that FLH of Northwest China has increased at a rate of approximate 1.2 gpm (geopotential meters) per year, which is statistically significant at the 0.01 level. Most grid boxes in Northwest China show consistent increasing trends, except the northern Tibetan Plateau. Periodic analyses demonstrate that primary period of FLH in Northwest China is approximately 15 years, and the different climate zones (eastern monsoon region, northwest arid region and Tibetan cold region) show similar periods. FLH is significantly related to surface air temperature during the study period ($r = 0.90$), especially in northwest arid region. The correlation coefficients are relatively higher in the colder months and lower in the hotter months. Altitude also correlates with mean FLH positively ($r = 0.64$) and trend magnitude in FLH negatively ($r = -0.63$).

1. Introduction

Free-air freezing level height (FLH) is an important parameter affecting hydrological and meteorological process (Diaz and Graham, 1996; Bradley et al., 2009). Previous studies showed that FLH changes can sensitively reflect the regional climate pattern, which is less influenced by the local destabilization than other ground-observed factors (Free and Seidel, 2005; Q. Zhang et al., 2010; G. Zhang et al., 2010). With climate warming in the past several decades (Solomon et al., 2007; Herman et al., 2010), most regions in China have experienced great climate changes (You et al., 2010; G. Sun et al., 2010; Li et al., 2009; Jones et al., 2008), which also can be exhibited in free-air temperature. In the past decade, more and more investigation focused on the long-term FLH change in China. Mu and Wang (2010) showed that the increasing of FLH since 1970 in China is associated with ground air temperature and atmospheric vapor. Based on 116 observational stations in China, Guo and Ding (2009) found that atmospheric temperature below 400 hPa has significantly increased during 1958–2005.

Northwest China is sensitive to climate change in the past century, which is shown in many researches (e.g. Shi et al., 2007; Q. Zhang et al., 2010; G. Zhang et al., 2010; Wang et al., 2011, 2012, 2013; Xu et al., 2011; Li et al., 2012a, 2012b, 2012c). According to the radiosonde data in Northwest China, the summer FLH correlates with ground air temperature (Huang et al., 2011). Xinjiang in Northwest has also experienced a generally increasing trend in FLH, but no abrupt change was detected (Zhang et al., 2005). Due to the altitude and latitude of Northwest China, many modern glaciers are distributed in the mountainous areas. Previous studies (Bradley et al., 2009) indicated that FLH at most regions in the tropics have increased in the past decades, and daily maximum temperature frequently is above freezing point at Quelccaya Icecap. Investigation on typical glaciers in China (Cheng et al., 2002; Zhang and Guo, 2011) also indicated a significant relationship between FLH and cryosphere. In addition, the water scarcity is an important issue for most regions in Northwest China. For inland rivers supplied mainly by meltwater from glaciers and snow, annual runoff is significantly related with summer FLH (Wang et al., 2008; Gong et al., 2010; Q. Zhang et al., 2010; G. Zhang et al., 2010; Qin et al., 2011). So, the daily FLH can be used for discharge prediction and flash flood warning in this region (Fu et al., 2011; Mao et al., 2007; H. Sun et al., 2010). According to the research of Chen et al. (2012),

* Corresponding author.
E-mail address: xyhuang0529@sina.cn (X. Huang).

1040-6182/$ – see front matter © 2013 Elsevier Ltd and INQUA. All rights reserved.
http://dx.doi.org/10.1016/j.quaint.2013.07.200

the sensitivity of runoff to FLH is related to the percentage of meltwater supplies.

The previous studies were mainly based on sounding data in the past decades. However, inhomogeneity may widely exist in the observed radiosonde data in China. It is necessary to assess the reliability of original data, using reanalysis data or other method. In this paper, the spatio-temporal changes in FLH in Northwest China during 1960–2012 were analyzed based on the NCEP/NCAR reanalysis, in order to provide more information on regional climate change.

2. Data and method

The original monthly data from 1960 to 2012 were acquired from NCEP/NCAR reanalysis dataset with a spatial resolution of 2.5° × 2.5°. This dataset was widely applied in FLH calculation in previous investigations (Harris et al., 2000; Thurai et al., 2003). In this study, neighboring levels were examined for a potential transition from a temperature below 0 °C to a temperature at or above 0 °C. Monthly FLH was calculated using linear interpolation between the geopotential heights of the corresponding levels. The calculated FLHs are expressed as geopotential meters (gpm).

Northwest China in this study includes Gansu Province, Shaanxi Province, Qinghai Province, Ningxia Hui Autonomous Region and Xinjiang Uygur Autonomous Region, covering an area of 3.1×10^6 km^2. Within Northwest China, 52 grid boxes in the NCEP/NCAR reanalysis were selected in the study area (Fig. 1). Due to the latitude ranges, the ground air temperature in Northwest China is relatively low in the winter half year, and FLH does not exist above ground level from November to March generally. The calculated month in this study is from April to October, and the arithmetic mean values of FLH in these seven months are considered as the annual series. Based on the climate zoning of China (Zhao et al., 1983), Northwest China can be subdivided into three subregions: eastern monsoon region, northwest arid region, and Tibetan cold region.

The NCEP-NCAR reanalysis were derived from an assimilation and modeling procedure that incorporated conventional and satellite observations (Kistler et al., 2001). However, previous research indicated that the inhomogeneity may still exist to some degree especially in western China (Ma et al., 2008). In this study, homogeneity was assessed using a penalized maximal *F* test (PMFT), and detected step changes were adjusted (Wang, 2008).

The nonparametric Sen's method is used to calculate the linear trends for FLH during the study period (Sen, 1968). The anomalies series is calculated according to the mean value during 1981–2010. Wavelet analysis is applied to reveal periodic features of FLH change and detect periodic variation (Torrence et al., 1998).

3. Results

3.1. Temporal changes in freezing level heights

Table 1 demonstrates the decadal change in FLH during the study period, and the regional mean series are exhibited as anomalies. The anomalies in the 2000s (including the early-2010s) are positive (17.1 gpm respectively), and the previous four decades from 1960 to 1999 show negative anomalies. Generally, FLH has shown an increasing trend during the period 1960–2012.

Table 1
Inter-decadal anomaly of free-air freezing level heights (FLH) in Northwest China and three climatic zones.

Study period	Anomaly (gpm)			
	Northwest China	Eastern monsoon region	Northwest arid region	Tibetan cold region
1960–1969	−24.1	−83.8	−66.2	62.2
1970–1979	−15.4	−43.1	−27.9	14.2
1980–1989	−17.3	−21.5	−36.8	13.8
1990–1999	−3.3	−23.7	−2.2	3.0
2000–2012	17.1	26.7	30.6	−6.8

As is shown in Table 1, the trends in FLH of eastern monsoon region and northwest arid region are generally similar with the regional mean trends of Northwest China, and positive anomalies can be found only in the 2000s (26.7 and 30.6 gpm for eastern monsoon region and northwest arid region, respectively). However, the anomalies of Tibetan cold region show an obviously different trend. The variation range of FLH in eastern monsoon region is the most significant among the three zones, and the range between the maxima and minima is more than 100 gpm.

Fig. 2 shows the long-term changes in FLH for the entire region and three climatic zones, respectively. Similar as the inter-decadal

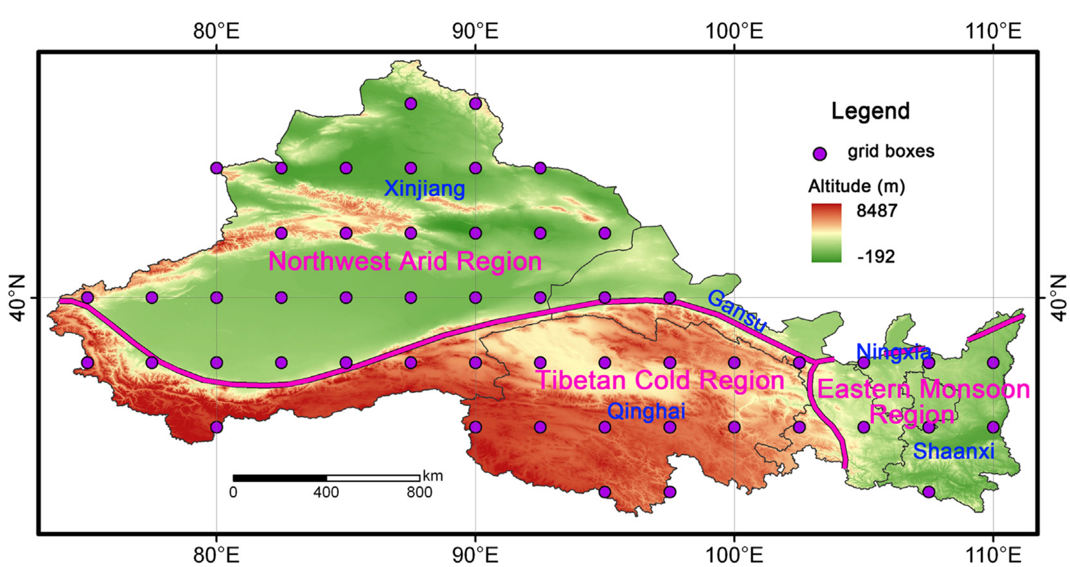

Fig. 1. Distribution of grid boxes in NCEP/NCAR reanalysis in Northwest China.

features shown in Table 1, increasing trends in FLH can be found for each series except in the Tibetan cold region during the study period. FLH have increased by 1.2 gpm per year in Northwest China during the period 1960–2012, which is statistically significant at the 0.01 level. The trends are consistent with climate warming, which is a synchronous performance as the ground air temperature increasing. According to previous research (Li et al., 2012a, 2012b, 2012c), the temperature rising in northwest arid region is more significant than the national mean and even the global mean. The trend magnitudes of FLH in eastern monsoon region and northwest arid region are 2.3 and 2.4 gpm per year, respectively, which is significant at the 0.001 level. The FLH in Tibetan cold region have decreased by −1.5 gpm per year, which is different from the other series.

The climate pattern in Northwest China experienced a significant transformation from warm-dry mode to warm-wet mode around the late 1980s (Shi et al., 2007). To focus on the recent climate change, FLH during the period 1990–2012 is also calculated, as shown in blue lines (in the web version) in Fig. 2. FLH in Northwest China and different natural zones all show increasing trends. This indicates a significant warming during recent decades.

3.2. Spatial changes in freezing level heights

Fig. 3 shows the spatial patterns of FLH changes at each grid box in Northwest China during 1960–2012. For the annual pattern in Fig. 3a, 58% of grid boxes show positive trends, and 42% shows negative trends. FLH at most areas of eastern monsoon region and northwest arid region have increased during 1960–2012. 86% of grid boxes in eastern monsoon region shows increasing trends, and 74% of grid boxes show increasing trends in the northwest arid region. FLH at most areas of Tibetan cold region have decreased during 1960–2012: 22% of grid boxes show positive trends, and 78% show negative trends. Altai Mountains in the northern section of northwest arid region is the area with the highest increment.

In April (Fig. 3b), 60% of grid boxes show increasing trends in Northwest China, and the spatial distribution of FLH is similar as the annual series. In May (Fig. 3c), the percentage of positive trends is 86% and 74% and 33% for eastern monsoon region, northwest arid region and Tibetan cold region respectively. In June (Fig. 3d), the percentage of negative trends in Tibetan cold region is 67%. In July (Fig. 3e), 54% of grid boxes shows increasing trends in Northwest China, and the percentage of positive trends are 57%, 78% and 17% for eastern monsoon region, northwest arid region and Tibetan cold region, respectively. In August (Fig. 3f), 50% of grid boxes show increasing trends in Northwest China, and the percentage of positive trends are 71% and 70% for the eastern monsoon region and northwest arid region, respectively. In September (Fig. 3g), 21% of grid boxes shows decreasing trends in Northwest China, and the percentage in Tibetan cold region is up to 44%. In October (Fig. 3h), 52% of grid boxes show increasing trends in Northwest China, and the percentage of positive trend is 6% for Tibetan cold region. Generally, FLH at most areas in eastern monsoon region and

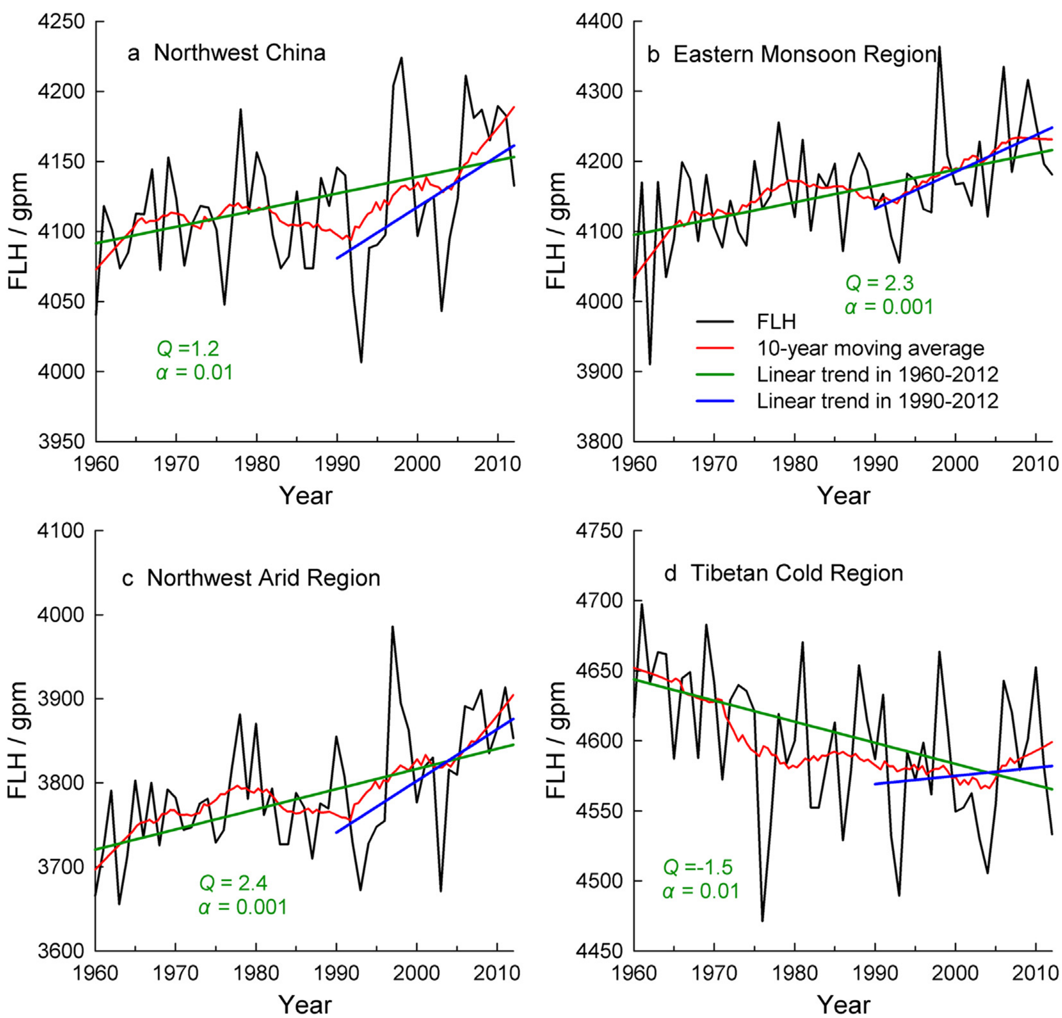

Fig. 2. Annual variation of free-air freezing level heights (FLH) for different natural zones in Northwest China during 1960–2012.

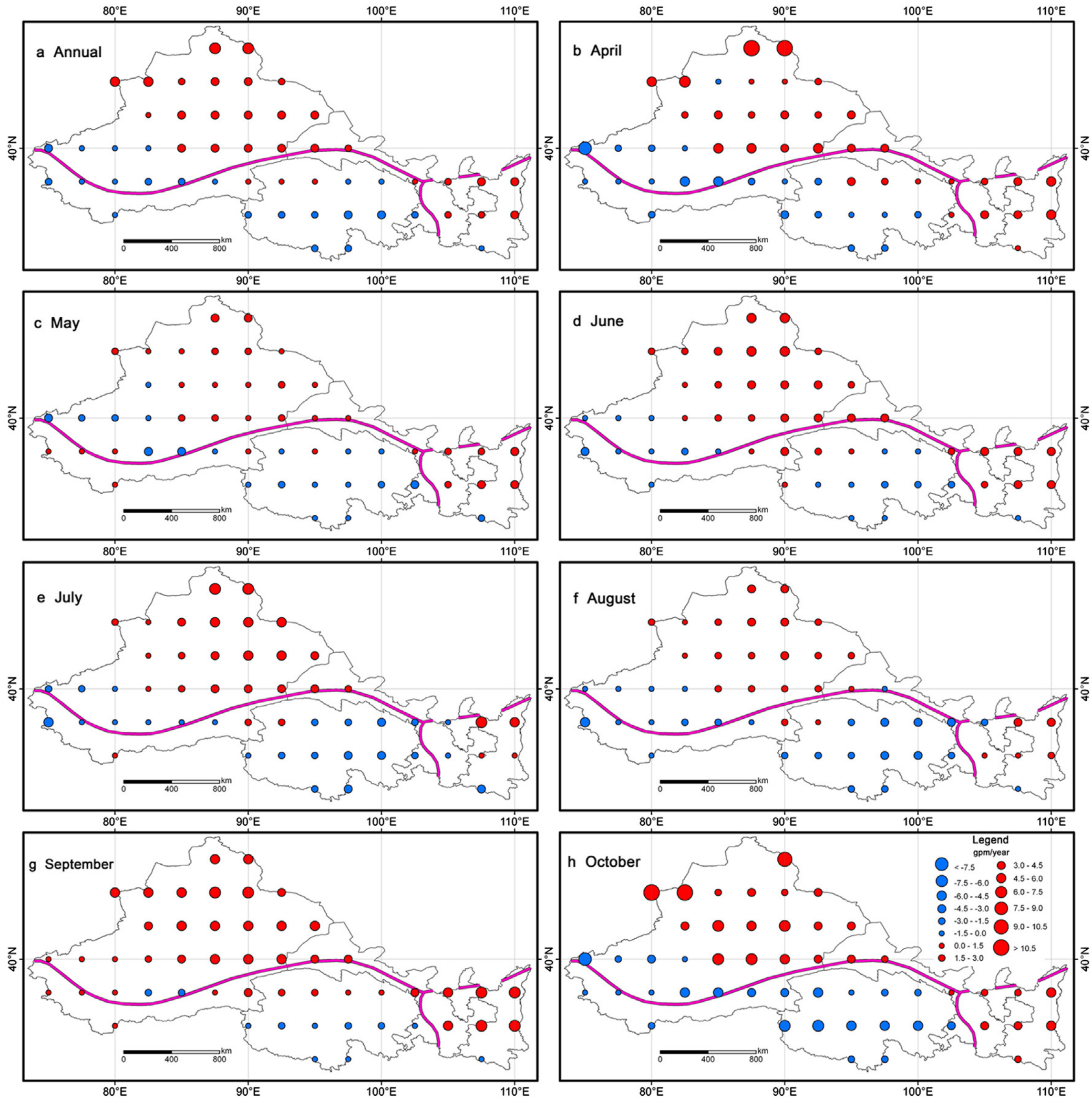

Fig. 3. Spatial distribution of linear trends of free-air freezing level heights (FLH) in Northwest China for annual and monthly series during 1960–2012.

northwest arid region has increased in most months, but FLH in Tibetan cold region has slightly decreased.

3.3. *Periodic analyses of freezing level heights*

Fig. 4a shows the contours of the real part of Morlet wavelet coefficients for the mean FLH in Northwest China. Periods of approximately 5 and 15 years are detected during the study period. Since the 1980s, there is a period of approximately 15 years with three significant suppressed centers (1960–1965, 1993–1996 and 2003–2005) and an enhanced center (1997–2002). According to the wavelet variances (Fig. 4b), two peaks can be detected, corresponding to the above-mentioned periods. The primary period is approximately 15 years, and the second period is approximately 5 years.

Fig. 5 shows the contours of real part of Morlet wavelet coefficients and wavelet variances for the mean FLH for different natural zones. For the annual FLH series in eastern monsoon region (Fig. 5a), periods of approximately 5 and 16 years can be found since 1960. There are two significant suppressed centers (1960–1965 and 2003–2007) and two enhanced center (1965–1970 and 2007–2012). As is shown in Fig. 5b, two peaks are detected in the wavelet variances. The primary period is approximately 16 years, and the second period is approximately 6 years.

FLH in northwest arid region (Fig. 5c) demonstrates an approximate 5-year period after 1995, and an approximate 16-year period before 1975 and after 1985. There are two significant suppressed centers (1960–1965 and 2003–2007) and two enhanced centers (1997–2001 and 2007–2012). The wavelet variances (Fig. 5d) also shows two peaks (approximate 5-year and 16-year periods), and the latter is the primary period.

For the annual FLH series in Tibetan cold region (Fig. 5e), a significant approximately 13-year period can be found during 1960–2012. Additionally, there are an approximately 8-year period in 1965–1980 and an approximate 5-year period after 1977. Two suppressed centers (1993–1996 and 2002–2005) and three enhanced centers (1988–1992, 1997–2001 and 2007–2010) can be found. Two peaks can be detected from the wavelet variances (Fig. 5f), which correspond to the 5-year and 13-year periods, respectively. The period of 13 years is the primary period.

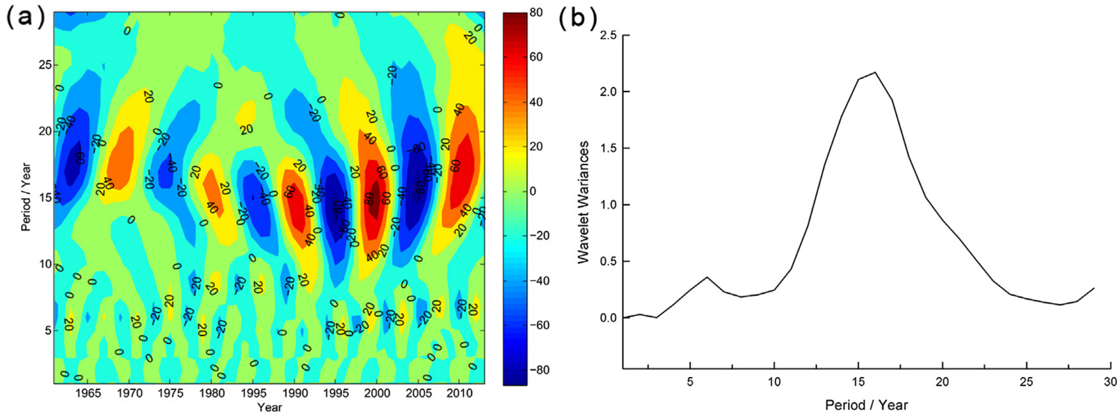

Fig. 4. Contours of real part of Morlet wavelet coefficients (a), and wavelet variances (b) of the mean free-air freezing level heights (FLH) in Northwest China from 1960 to 2012.

Therefore, both eastern monsoon region and northwest arid region all exhibit periods of approximately 5 and 16 years, and the 16-year period is the primary period. In Tibetan cold region, the primary period is approximately 13 years.

3.4. Relationship between FLH and surface temperature

Previous research indicated that FLH increase is considered to be related to surface air temperature increase (Huang et al., 2011). Based on the NCEP/NCAR reanalysis, we calculate the correlation coefficients between FLH and surface temperature on an annual and monthly basis (Table 2). For the annual relationships in Northwest China, FLH significantly correlates with surface temperature ($\alpha = 0.01$), and the correlation coefficients is 0.90. This indicates that free-air FLH increases with the rise of surface temperature. The coefficients during different months range from 0.72 (August) to 0.98 (April). During the summer half year, the correlation coefficients are relatively higher in the colder months, and are lower in the hotter months (i.e. July and August).

Table 2
Correlation coefficients between free-air freezing level heights (FLH) and surface air temperature in Northwest China and three climatic zones.

Month	Northwest China	Eastern monsoon region	Northwest arid region	Tibetan cold region
April	0.98**	0.81**	0.97**	0.93**
May	0.94**	0.48**	0.92**	0.95**
June	0.89**	0.22	0.89**	0.84**
July	0.77**	0.25	0.76**	0.80**
August	0.72**	0.41**	0.74**	0.79**
September	0.90**	0.48**	0.86**	0.92**
October	0.93**	0.63**	0.92**	0.89**
Annual	0.90**	0.22	0.90**	0.55**

Note: * and ** denote statistically significant at the 0.05 and 0.01 levels.

Insignificant positive correlations between FLH and surface temperature are examined for eastern monsoon region, and the correlation coefficients is only 0.22. On a monthly basis, the coefficient in April is 0.81 ($\alpha = 0.01$), which is the largest for each month. In June and July, the coefficients are not statistically significant. From August to October, the coefficients have increased from 0.41 to 0.63, which are significant at the 0.01 level.

For northwest arid region and Tibetan cold region, all the correlations between FLH and surface temperature range from 0.74 to 0.97, and are all statistically significant at the 0.01 level. The maximum coefficients occur in April ($r = 0.97$) and May ($r = 0.95$) for northwest arid region and Tibetan cold region, respectively. The minimum coefficients both occur in August for the two subregions.

3.5. Relationship between FLH and altitude

Mean FLH shows negative correlations with altitude for each grid box in the study area, and the correlation coefficient is 0.64 on an annual basis which is statistically significant at the 0.01 level (Table 3). On a monthly basis, correlation coefficients between altitude and mean FLH range from 0.56 to 0.69. All the correlations are statistically significant at the 0.01 level. During the colder months (e.g. April, May and October), the coefficients are generally lower. And the maximum coefficient occur in June ($r = 0.69$).

Table 3
Correlation coefficients between altitude and free-air freezing level heights (FLH) or trend magnitudes of FLH.

Month	Mean FLH	Trend magnitude of FLH
April	0.56**	−0.43**
May	0.64**	−0.42**
June	0.69**	−0.59**
July	0.66**	−0.62**
August	0.66**	−0.64**
September	0.67**	−0.65**
October	0.56**	−0.59**
Annual	0.64**	−0.63**

Note: * and ** denote statistically significant at the 0.05 and 0.01 levels.

In addition, altitude and trend magnitudes in FLH also show high correlations ($r = -0.63$, $\alpha = 0.01$). On a monthly basis, the minimum correlation coefficient between altitude and trend magnitude of FLH occur in September ($r = -0.65$), and the maximum coefficient occur in May ($r = -0.42$). Correlations in different months are statistically significant at the 0.01 level. Generally, for the regions with higher altitude, mean FLH is relatively higher, and the trend magnitude is lower. The low-altitude areas have suffered low FLH and high FLH trend magnitude during the study period. In the hotter months, the correlations are more significant than those in the colder months.

4. Summary and discussion

During the period 1960–2012, free-air freezing level height in Northwest China shows a significantly increasing trend at averagely 1.2 gpm per year. The mean increments at the northwest arid region are larger than those at the Tibetan cold region and eastern monsoon region. On a spatial basis, most grid boxes of Northwest China show positive trends in FLH, except the northern Tibetan Plateau.

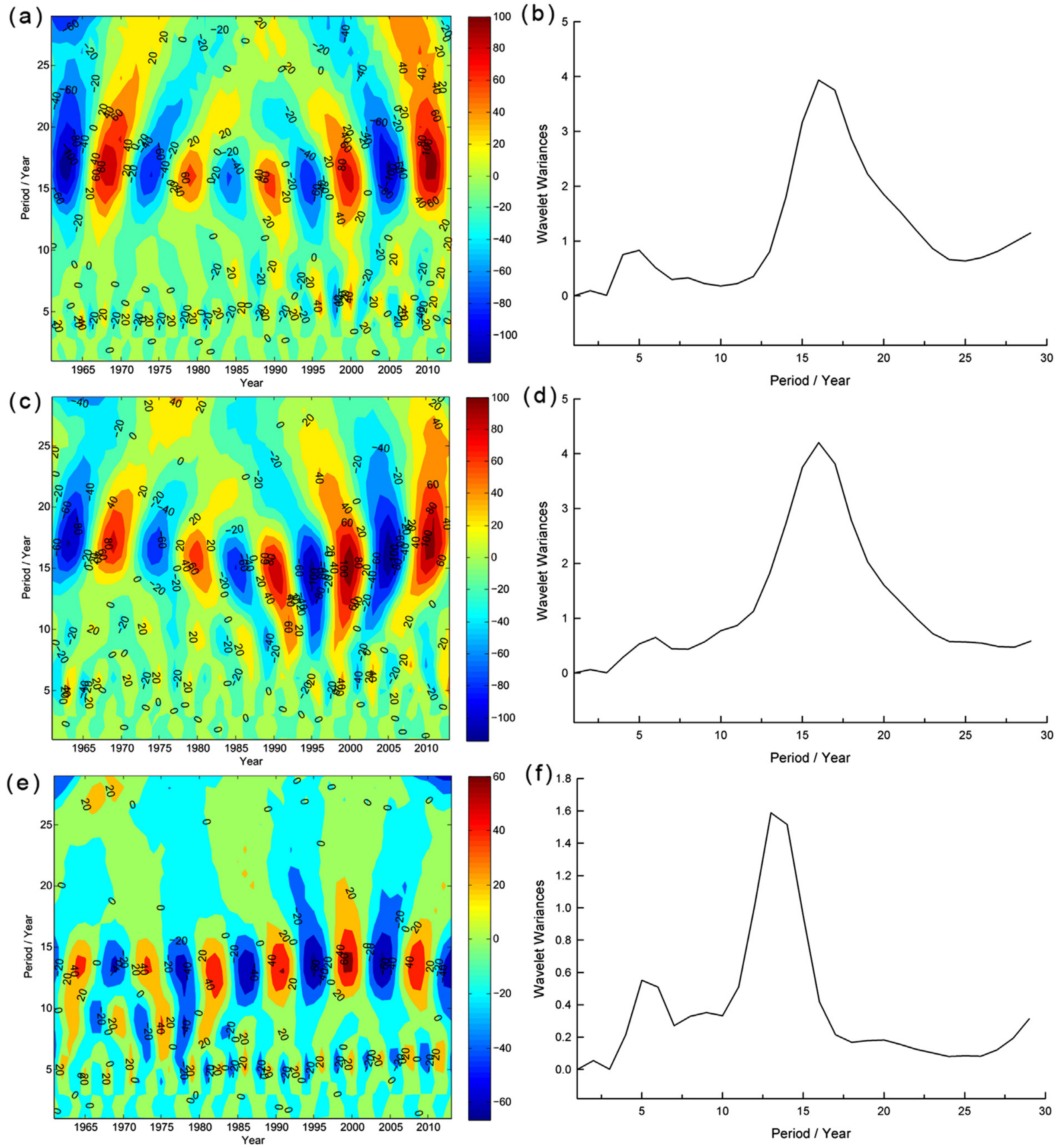

Fig. 5. Contours of real part of Morlet wavelet coefficients (a, c, e), and wavelet variances (b, d, f) of the mean free-air freezing level heights (FLH) for different natural zones in Northwest China from 1960 to 2012.

The regional warming is related to large-scale atmospheric circulation (You et al., 2010). Previous investigation shows that the weakening of the Siberian High in the 1980s to 1990s and the increasing of greenhouse gas emission is the main reason for the rapidly increasing temperature in northwest China (Li et al., 2012a). In this study, the significant correlation between FLH and surface air temperature can be found ($r = 0.90$), especially in northwest arid region. During the period 1960–2012, FLH shows an increasing trend, which is consistent with surface warming. The correlation coefficients are higher in the colder months, which may be related to the lower FLH near ground surface in these periods.

In addition to the atmospheric circulation, mean FLH and the trend magnitudes are also influenced by other factors. Altitude correlates with mean FLH positively ($r = 0.64$) and trend magnitude in FLH negatively ($r = -0.63$). The increasing trends in FLH are more significant for the low-lying areas, and the low-altitude regions generally have low FLH. In addition, the cloud amount, solar radiation and underlying surface may also be related with free-air freezing level (Jensen and Del Genio, 2006; Medvigy and Beaulieu, 2012), which needs further investigation.

With climate warming in the past several decades, Northwest China has experienced a great change in climate and environment. Long-term variations in the free-air temperature and freezing level heights may provide meaningful information about climate change in the past half century. Due to the distribution of modern glaciers and high-altitude cryosphere in Northwest China, the variability of free-air freezing level may have great impact on regional water resources. The current warming trends exhibited as increased FLH in Northwest China effectively contribute to the rapid shrinkage of glaciers in the past decades.

Acknowledgments

This study was supported by the Special Fund for Meteorological Scientific Research in the Public Interest (No. GYHY201006023), the National Natural Science Foundation of China (No. 41175081) and the Scientific Research Project for Master in Lanzhou Institute of Arid Meteorology, China Meteorological Administration (No. KYS2012SSKY06).

References

Bradley, R.S., Keimig, F.T., Diaz, H.F., Hardy, D.R., 2009. Recent changes in freezing level heights in the tropics with implications for the deglacierization of high mountain regions. Geophysical Research Letters 36, L17701. http://dx.doi.org/10.1029/2009GL037712.

Chen, Z.S., Chen, Y.N., Li, W.H., 2012. Response of runoff to change of atmospheric 0 °C level height in summer in arid region of Northwest China. Science China: Earth Sciences 55, 1533–1544.

Cheng, Y., Li, D., Hu, W., Sheng, F., 2002. Relationship between glacial thaw of Qilian Mountain and upper temperature. Plateau Meteorology 21, 217–221 (in Chinese).

Diaz, H.F., Graham, N.E., 1996. Recent changes in tropical freezing heights and the role of sea surface temperature. Nature 383, 152–155.

Free, M., Seidel, D.J., 2005. Causes of differing temperature trends in radiosonde upper air data sets. Journal of Geophysical Research Atmospheres 110, D07101. http://dx.doi.org/10.1029/2004JD005481.

Fu, H., Jia, L., Xiao, J., Li, C., Feng, Z., 2011. Classification of snowmelt flood and analysis on its formation causes in the Kumalak River Basin. Arid Zone Research 28, 433–437 (in Chinese).

Gong, H., Shi, Y., Feng, Z., 2010. Relationship between the 0 °C layer height and the streamflow of the Urumqi River in the period of spring snowmelt. Arid Zone Research 27, 69–74 (in Chinese).

Guo, Y., Ding, Y., 2009. Long-term free-atmosphere temperature trends in China derived from homogenized in situ radiosonde temperature series. Journal of Climate 22, 1037–1051.

Harris, G.N., Bowman, K.P., Shin, D., 2000. Comparison of freezing-level altitudes from the NCEP Reanalysis with TRMM precipitation radar brightband data. Journal of Climate 13, 4137–4148.

Herman, B.M., Brunke, M.A., Pielke Sr., R.A., Christy, J.R., McNider, R.T., 2010. Satellite global and hemispheric lower tropospheric temperature annual temperature cycle. Remote Sensing 2, 2561–2570.

Huang, X., Zhang, M., Wang, S., Li, Y., Pan, S., 2011. Variation of 0 °C isotherm height and ground temperature in summer during the past 50 years in northwest China. Acta Geographica Sinica 66, 1191–1199 (in Chinese).

Jensen, M.P., Del Genio, A.D., 2006. Factors limiting convective cloud-top height at the ARM Nauru Island Climate Research Facility. Journal of Climate 19, 2105–2117.

Jones, P.D., Lister, D.H., Li, Q., 2008. Urbanization effects in large-scale temperature records, with an emphasis on China. Journal of Geophysical Research 113, D16122. http://dx.doi.org/10.1029/2008/JD009916.

Kistler, R., Kistler, R., Kalnay, E., Collins, W., Saha, S., White, G., Woollen, J., Chelliah, M., Ebisuzaki, W., Kanamitsu, M., Kousky, V., van den Dool, H., Jenne, R., Fiorino, M., 2001. The NCEP-NCAR 50-year reanalysis: monthly means CD-ROM and documentation. Bulletin of the American Meteorological Society 82, 247–267.

Li, B., Chen, Y., Shi, X., 2012a. Why does the temperature rise faster in the arid region of northwest China. Journal of Geophysical Research 117, D16115. http://dx.doi.org/10.1029/2012JD017953.

Li, B., Chen, Y., Shi, X., Chen, Z., Li, W., 2012b. Temperature and precipitation changes in different environments in the arid region of northwest China. Theoretical and Applied Climatology. http://dx.doi.org/10.1007/s00704-012-0753-4.

Li, Q., Zhang, H., Liu, X., Chen, J., Li, W., Jones, P., 2009. A mainland China homogenized historical temperature dataset of 1951–2004. Bulletin of the American Meteorological Society 90, 1062–1065.

Li, Z., Chen, Y., Yang, J., Wang, Y., 2012c. Potential evapotranspiration and its attribution over the past 50 years in the arid region of Northwest China. Hydrological Processes. http://dx.doi.org/10.1002/hyp.9643.

Ma, L., Zhang, T., Li, Q., Frauenfeld, O.W., Qin, D., 2008. Evaluation of ERA-40, NCEP-1, and NCEP-2 reanalysis air temperatures with ground-based measurements in China. Journal of Geophysical Research 113. http://dx.doi.org/10.1029/2007JD009549.

Mao, W., Yusup, A., Cheng, P., Dong, K., 2007. Extreme flood events in 1999 and their formation conditions in northern slopes of the Middle Kunlun Mountains. Journal of Glaciology and Geocryology 29, 553–558 (in Chinese).

Medvigy, D., Beaulieu, C., 2012. Trends in daily solar radiation and precipitation coefficients of variation since 1984. Journal of Climate 25, 1330–1339.

Mu, L., Wang, Y., 2010. Study on causes of freezing level height increasing in China by the adiabatic atmospheric model. College Physics 29, 46–47, 51 (in Chinese).

Qin, Y., Liu, Z., Lu, Z., Wei, Z., 2011. Calculation of runoff series in ungauged basins from the 0 °C level height in summer: a case of Ruoqiang River Basin. Arid Land Geography 34, 278–283 (in Chinese).

Sen, P.K., 1968. Estimates of the regression coefficient based on Kendall's tau. Journal of the American Statistical Association 63, 1379–1389.

Shi, Y., Shen, Y., Kang, E., Li, D., Ding, Y., Zhang, G., Hu, R., 2007. Recent and future climate change in northwest China. Climate Change 80, 379–393.

Sun, G., Chen, Y., Li, W., Wang, Y., Yang, Y., 2010. The response of glacial lake outburst floods to climate change in the Yarkant River, Xinjiang. Journal of Glaciology and Geocryology 32, 580–586 (in Chinese).

Sun, H., Chen, Y., Li, W., Li, F., Chen, Y., Hao, X., Yang, Y., 2010. Variation and abrupt change of climate in Ili River Basin, Xinjiang. Journal of Geographical Sciences 20, 652–666.

Thurai, M., Deguchi, E., Iguchi, T., Okamoto, K., 2003. Freezing height distribution in the tropics. International Journal of Satellite Communications and Networking 21, 533–545.

Torrence, C., Compo, G.P., 1998. A practical guide to wavelet analysis. Bulletin of the American Meteorological Society 79, 61–78.

Wang, H., Chen, Y., Chen, Z., 2012. Spatial distribution and temporal trends of mean precipitation and extremes in the arid region, northwest of China, during 1960–2010. Hydrological Processes. http://dx.doi.org/10.1002/hyp.9339.

Wang, H., Chen, Y., Xun, S., Lai, D., Fan, Y., Li, Z., 2013. Changes in daily climate extremes in the arid area of northwestern China. Theoretical and Applied Climatology 112, 15–28.

Wang, S., Zhang, M., Li, Z., Wang, F., Li, H., Li, Y., Huang, X., 2011. Glacier area variation and climate change in the Chinese Tianshan Mountains since 1960. Journal of Geographical Sciences 21, 263–273.

Wang, X.L., 2008. Accounting for autocorrelation in detecting mean shifts in climate data series using the penalized maximal *t* or *F* test. Journal of Applied Meteorology and Climatology 47, 2423–2444.

Wang, Y., Yusup, A., Ma, H., Mao, W., 2008. Response of summer average discharge in the Hotan River to changes in regional 0 °C level height. Advances in Climate Change Research 4, 151–155 (in Chinese).

Xu, J., Chen, Y., Lu, F., Li, W., Zhang, L., Hong, Y., 2011. The nonlinear trend of runoff and its response to climate change in the Aksu River, western China. International Journal of Climatology 31, 687–695.

You, Q., Shi, C., Aguilar, E., Pepin, K., Flügel, W.-A., Yan, Y., Xu, Y., Zhang, Y., Huang, J., 2010. Changes in daily climate extremes in China and its connection to the large scale atmospheric circulation during 1961–2003. Climate Dynamics 36, 2399–2417.

Zhang, G., Yang, L., Yang, Q., 2005. Changing trend and abrupt change of the 0 °C level height in summer in Xinjiang from 1960 to 2002. Journal of Glaciology and Geocryology 27, 376–380 (in Chinese).

Zhang, Q., Xu, C.Y., Tao, H., Jiang, T., Chen, Y.D., 2010. Climate changes and their impacts on water resources in the arid regions: a case study of the Tarim River Basin, China. Stochastic Environmental Research and Risk Assessment 24, 349–358.

Zhang, G., Sun, S., Ma, Y., Zhao, L., 2010. The response of annual runoff to the height change of the summertime 0 °C level over Xinjiang. Journal of Geographical Sciences 20, 833–847.

Zhang, Y.S., Guo, Y., 2011. Variability of atmospheric freezing-level height and its impact on the cryosphere in China. Annals of Glaciology 52, 81–88.